Nature Communications

https://doi.org/10.1038/s41467-026-73737-2

Article in Press

# Impact of air-ice $CO_2$ fluxes on polar ocean carbon budgets from a bipolar data compilation

Received: 4 February 2026

Accepted: 18 May 2026

Cite this article as: Crabeck, O., Nomura, D., Djeutchouang, L.M. *et al.* Impact of air-ice $CO_2$ fluxes on polar ocean carbon budgets from a bipolar data compilation. *Nat Commun* (2026). https://doi.org/10.1038/s41467-026-73737-2

**Odile Crabeck, Daiki Nomura, Laique M. Djeutchouang, Victoria R. Dutch, Sebastien Moreau, G. T. Else Brent, Lisa A. Miller & Bruno Delille**

# sImpact of air-ice $CO_2$ fluxes on polar ocean carbon budgets from a bipolar data compilation

Odile Crabeck[1,2*], Daiki Nomura[3*], Laique M. Djeutchouang[4,5,6], Victoria R. Dutch[7,8],Sebastien Moreau[9], Brent G.T. Else[10], Lisa A. Miller[11], Bruno Delille[1]

[1]Chemical Oceanography Unit, Science Faculty, University of Liège, Liège, Belgium
[2]Department of Geosciences, Environment and Society, Université Libre de Bruxelles, Brussels, Belgium
[3]Hokkaido University, Hakodate, Japan
[4]School for Climate Studies, Stellenbosch University, Stellenbosch, South-Africa
[5]Southern Ocean Carbon – Climate Observatory, CSIR, Cape Town, South-Africa
[6]Engr. Computer Science, University of California, Davis, USA
[7]Centre for Ocean & Atmospheric Sciences, School of Environmental Sciences, University of East Anglia, Norwich, UK
[8]Department of Earth Sciences, Oxford University, Oxford, UK.
[9]Norwegian Polar Institute, Tromsø, Norway
[10]Department of Geography, University of Calgary, Calgary, AB, Canada
[11]Institute of Ocean Sciences, Fisheries and Oceans Canada, Sidney, BC, Canada

[*]Corresponding authors: ocrabeck@uliege.be, daiki.nomura@fish.hokudai.ac.jp

**Abstract**

In ocean carbon budget assessments, sea ice is still treated as an impermeable barrier, rather than a dynamic interface mediating $CO_2$ exchange between ocean and atmosphere. We compiled more than 6000 chamber-based air–ice $CO_2$ flux measurements from the Arctic and Southern Oceans between 2003 and 2021, spanning diverse ice, snow, and seasonal conditions. These data show that sea ice releases $CO_2$ in winter and absorbs it in summer, with summer uptake offsetting winter emissions. On an annual basis, sea ice represents a small net $CO_2$ source of +4 Tg C $yr^{-1}$ in the Arctic and +2 Tg C $yr^{-1}$ in the Southern Ocean, challenging earlier views of a major sink. Although these fluxes are negligible at basin scales relative to open-ocean uptake, sea ice exchanges gases even in cold winter conditions, with implications for small-scale processes and other trace gases, underscoring the need for sustained, process-resolving observations.

## 1. Introduction

Sea ice is a defining feature of the Arctic and Southern Oceans, shaping their physical, chemical, and biological processes[1–4]. Early studies primarily viewed sea ice as an inert and impermeable physical barrier separating the ocean from the atmosphere, thereby largely inhibiting gas exchange. This perception has influenced both scientific understanding and the development of global climate models[5–7].

A major paradigm shift began in the 1960s when researchers discovered that sea ice contains a complex network of brine channels and air pockets and is permeable under a wide

range of conditions [8–12]. Research over the last couple of decades has revealed that sea ice is not merely a passive barrier, but an active participant in carbon and nutrient cycling, confirming that carbon can be recycled through respiration and photosynthesis[13,14], be temporarily concentrated as dissolved inorganic carbon (DIC) in brine inclusions[13,15–22] and even precipitate as ikaite crystals[3,23–28]. New evidence has confirmed that sea ice contains gases both dissolved in brine and trapped as bubbles, and that these gases can be exchanged with the underlying seawater and the overlying atmosphere[29–33] with possible impacts on regional carbon budgets[34–36].

The first measurements of gas fluxes through sea ice were made in a laboratory in the mid-1970s[10], but it was not until 2002 that direct measurements were made in the field using eddy covariance (EC), a meteorological technique that utilizes high-frequency (10-20 Hz) measurements of vertical wind velocity and atmospheric carbon dioxide ($CO_2$) above the sea-ice surface[37,38]. These pioneering EC measurements were artificially high due to unexpected (and hence uncorrected) impacts of water vapor and sensible heat fluxes on calculated $CO_2$ fluxes, biases which were particularly pronounced in cold sea-ice environments where the $CO_2$ flux signal is generally small[39,40]. However, they sparked new research into $CO_2$ geochemistry in sea ice, profoundly advancing our understanding of this previously overlooked component of the global carbon cycle[4]. The complexity of EC measurements, as well as their associated uncertainties, contributed to the wider adoption of much simpler chamber measurements of air-ice $CO_2$ fluxes, despite their own limitations[41]. Today, air-ice $CO_2$ fluxes from EC measurements remain relatively limited in both time and space.

The flux chamber method involves placing a small enclosure (about 0.004 $m^3$ over an area of about 0.03 $m^2$) on the ice surface and measuring changes in the $CO_2$ concentration within the headspace over a short period of time (i.e., up to half an hour)[20]. The $CO_2$ flux is calculated from the change in the $CO_2$ concentration within the chamber (positive values indicate $CO_2$ released from the ice surface to the air) and the headspace volume and area enclosed by the chamber.

Field deployments have indicated that fluxes over sea ice can reach several mmol $CO_2$ $m^{-2}$ $day^{-1}$, with sea ice tending to release $CO_2$ during growth and take it up from the atmosphere during melt[18,19,42–45]. These findings led to the hypothesis that, given its vast spatial extent, sea ice could play a significant role in the polar oceans' carbon budget. Supporting this idea, Delille et al.[16] estimated, based on sparse data, that air-ice $CO_2$ fluxes could account for up to 58% of the annual $CO_2$ uptake by the Southern Ocean.

Despite these insights, the contribution of sea ice remains largely ignored in current estimates of the polar ocean carbon budget[46–50] and is still neglected in Earth system models, which typically treat sea ice as impermeable to gas transfer. Over the past two decades, however, systematic measurements of air–ice $CO_2$ fluxes across diverse regions and seasons have provided new perspectives on the mechanisms and variability of these exchanges. This growing body of work now enables us to revisit long-standing assumptions and assess the true role of sea ice in the polar carbon cycle. By synthesizing these data, we can more conclusively determine whether sea ice acts as a net source or sink of $CO_2$ and quantify its contribution to the carbon budget of the polar oceans.

## 2. Results and discussion

### 2.1. Description of the database

We have compiled all available air–ice $CO_2$ fluxes measured using the chamber method. The database comprises 6298 individual air–ice $CO_2$ flux chamber measurements (Table 1) performed between 2003 and 2021 during 14 Arctic (4719 measurements) and 8 Antarctic campaigns (1579 measurements). The datasets cover every season in the Arctic and the Antarctic; however, with 80% and 60% of measurements during spring for the Arctic (April-June) and Southern (October-December) oceans, respectively, spring is the most extensively studied season (Fig. 1a). For the Southern Ocean, no data are available in March or August. The dearth of data in winter reflects the challenges of accessing sea ice under extreme conditions, while in summer and fall, low sea-ice concentrations limit sampling opportunities.

Approximately 50% of our measurements were taken over snow-covered sea ice, and 40% were taken on bare sea ice. In the last case, the snow was either absent or removed with a shovel, and the chamber was placed directly on the sea-ice surface. While the available metadata do not always allow for discrimination between the natural absence of snow or snow that has been deliberately removed, measurements taken over bare ice during winter months often include notes indicating that the snow cover had been intentionally cleared. The last 10% of our measurements (Fig. 2b) covers sea-ice features such as melt ponds (pools of low salinity meltwater on the sea-ice surface during the summer months), slush (seawater-saturated snow at the sea-ice surface), and frost flowers (ice crystals growing on the surface of thin sea ice). The compiled datasets (Table 1, Fig. 1b) span most of the western Arctic and the circumpolar Southern Ocean and include first-year (FYI), multi-year (MYI), landfast and pack ice. Note that both landfast and pack ice can be either first- or multi-year. While we acknowledge that the coverage in time and space of our database is not fully representative of all Arctic and Antarctic sea-ice conditions, and that it is heavily biased towards some seasons and locations, this database offers a unique opportunity to derive monthly and yearly air–sea ice carbon fluxes in the Arctic and Southern Oceans. For consistency with the existing literature, we are reporting fluxes in units of mmol $m^{-2}$ $day^{-1}$ (i.e., implied to be representative of daily averages) throughout this paper, although the actual measurements are on timescales of only 20 to 30 minutes.

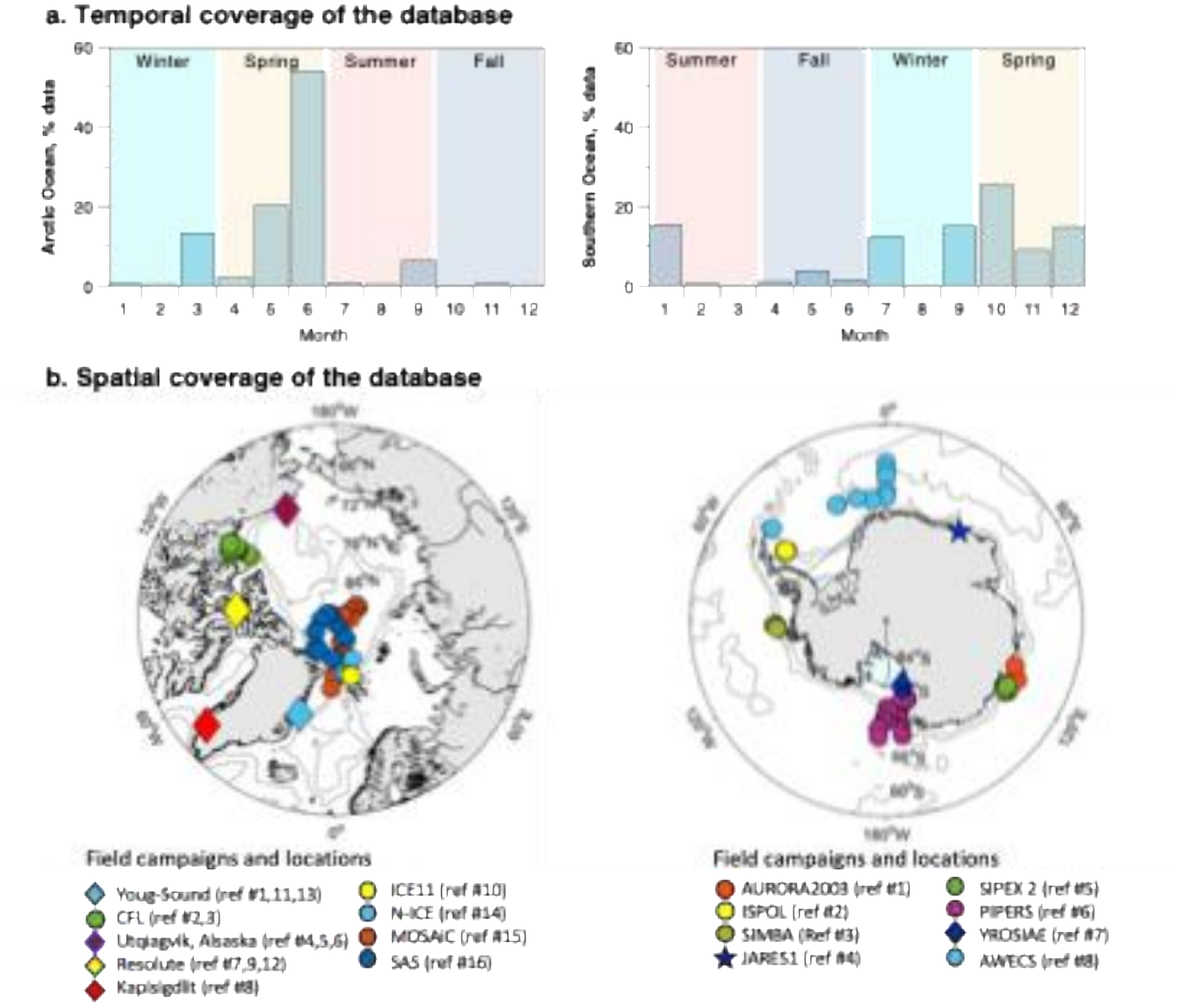


**Fig. 1 Spatial and temporal coverage of the data compilation.** (a) Seasonal representation of the dataset, percentage (%) of the measurements in each ocean collected during each month of the year. (b) Spatial distribution of the dataset. The number following each location references a field campaign listed in Table 1.

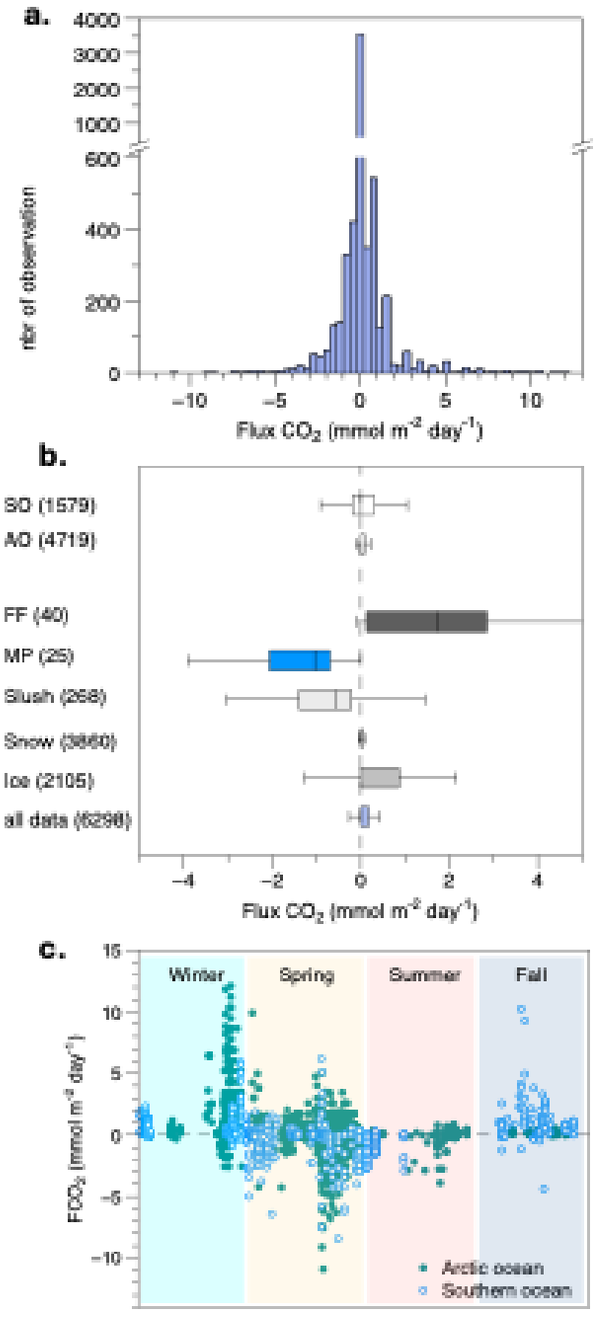


**Fig. 2: Key characteristics of the data compilation.** (a) Histogram of air–ice $CO_2$ fluxes in mmol $m^{-2}$ $day^{-1}$ , and (b) interquartile (IQ) box plot of air–ice $CO_2$ fluxes in mmol $m^{-2}$ $day^{-1}$ per ice type; the number in brackets is the number of measurements for each category (SO = Southern Ocean, AO = Arctic Ocean, FF = frost flowers, MP = melt pond). The centre line is the median, the limits of the box are the first (Q1) and third quartile (Q3), the whiskers are drawn to the smallest/largest non-outlier. Outliers are defined as either Q1-1.5 IQR or Q3+1.5 IQR. (c) Seasonal distribution of air–ice $CO_2$ fluxes in mmol $m^{-2}$ $day^{-1}$ for the Arctic and Southern Oceans. Positive fluxes indicate $CO_2$ transport to the atmosphere; negative fluxes indicate $CO_2$ uptake by the sea ice.

**Table 1.** List of measurements present in the database

| Ref Fig 1 | Reference -project | $CO_2$ Flux mmol $m^{-2}$ $day^{-1a}$ | Count | Month, year | Season | Region | Ice type |
|---|---|---|---|---|---|---|---|
| | | | **Arctic Ocean (n=4712)** | | | | |
| **1** | Sejr et al. (2011)[51] | 0.0 to +1.1 | 6 | Mar -Apr, 2003 | Spring | Young Sound, Greenland | Fast ice/ Thin |
| **2** | Else et al. (Unpub) CFL | 0.0 to +6.5 | 27 | Nov-Mar, 2007-08 | Fall-Winter | Amundsen Gulf | Fast ice |
| **3** | Geilfus et al. (2012)[19]CFL | –2.6 to +0.8 | 42 | Apr-Jun,2008 | Spring | Amundsen Gulf | Pack & Fast ice |
| **4** | Nomura et al. (2010)[45] | –1.0 to +0.7 | 8 | May, 2008 | Spring | Utqiagvik, Alaska | Fast ice |
| **5** | Geilfus et al. (2013)[52] | +4.2 to +9.9 | 4 | Apr, 2009 | Spring | Utqiagvik, Alaska | Fast ice/Thin |
| **6** | Delille et al. (Unpub) | –0.3 to +3.8 | 18 | Jan-Jun, 2009 | Winter-Spring | Utqiagvik, Alaska | Fast ice/ Thin |
| **7** | Fischer, (2013)[53] | –3.5 to +5.2 | 1065 | May-Jun, 2010 | Spring | Resolute Passage | Fast ice |
| **8** | Fischer, (2013)[53] | –2.2 to +12.1 | 492 | Mar, 2010 | Late Winter | Kapisigdlit, Greenland | Fast ice |
| **9** | Brown et al. (2015)[15] Arctic-ICE | –4.4 to +5.0 | 95 | May-Jun, 2011 | Spring | Resolute Passage | Fast ice |
| **10** | Nomura et al. (2013)[54] ICE11 | –1.2 to +0.1 | 86 | May, 2011 | Spring | North of Svalbard | Pack ice |
| **11** | Barber et al. (2014)[55] CERC | +3.0 to +3.7 | 32 | Mar, 2012 | Late Winter | Young Sound, Greenland | Frost Flower |
| **12** | Geilfus et al. (2015)[18] | –4.8 to 0.0 | 7 | Jun, 2012 | Late Spring | Resolute Passage | Meltpond |
| **13** | Geilfus et al. (2023)[56] | –10.9 to +0.5 | 2184 | Jun-Jul, 2014 | Summer | Young Sound, Greenland | Fast ice |
| **14** | Nomura et al. (2018)[20] NICE2015 | –0.8 to +11.8 | 151 | Jan-May, 2015 | Winter-Spring | North of Svalbard | Pack ice |
| **15** | Nomura et al. (2024)[57] MOSAiC | –3.9 to +3.2 | 490 | Sep-Aug, 2019-20 | Year-Round | Central Basin | FYI&MYI |
| **16** | Prytherch et al. (2024)[58] | –2.2 to +0.2 | 12 | Aug-Sep, 2021 | Summer | Central Basin | MYI |
| | | | **Southern Ocean (n=1579)** | | | | |
| **1** | Delille et al. (2014)[16] 2003/V1 | –1.0 to +1.9 | 8 | Sep-Oct, 2003 | Spring | Indian sector | Pack ice |
| **2** | Delille et al. (2014)[16] ISPOL | –5.5 to –2.0 | 39 | Nov-Dec, 2004 | Summer | Weddell Sea | Pack ice |
| **3** | Geilfus et al. (2014)[59] SIMBA | –2.9 to +0.3 | 69 | Oct, 2007 | Spring | Bellingshausen Sea | Pack ice |
| **4** | Nomura et al. (2013)[54] JARE51 | –2.3 to +0.1 | 276 | Jan-Feb, 2009-10 | Summer | Lützow-Holm Bay | Fast ice |
| **5** | Nomura et al. (Unpub) SIPEX2 | –1.0 to +0.8 | 330 | Sep-Oct, 2012 | Spring | Pacific sector | Pack ice |
| **6** | Van der Linden, (2021)[60] PIPERS | –4.4 to +10.3 | 86 | Apr-Jun, 2017 | Fall | Ross Sea West coast | Pack ice/Thin |
| **7** | Van der Linden et al. (2020)[13] YROSIAE | –9.7 to +6.2 | 555 | Sep-Dec, 2011-12 | Spring | Ross Sea Mc Murdo | Fast ice |
| **8** | Nomura et al. (Unpub) AWECS | +0.2 to +1.5 | 216 | Jun-Jul, 2013 | Winter | Weddell Sea | Pack ice |

[a]Although the actual measurements are on timescales of minutes, we represent fluxes in units of mmol $m^{-2}$ $day^{-1}$, for the sake of consistency with previously published literature.

### 2.2. Flux magnitudes and seasonality

The observed $CO_2$ fluxes range from –10.9 to +12.1 mmol $m^{-2}$ $day^{-1}$ (Fig. 2a, Table 1), showing a marked seasonality and strong dependence on sea-ice features such as melt ponds, frost flowers, and snow cover (Fig. 2b & c). Despite the large variability in flux magnitudes,

the dataset's mean (0.1±1.3 mmol $m^{-2}$ $day^{-1}$) and median (0.0 mmol $m^{-2}$ $day^{-1}$; IQR 0.0,+0.2) values highlight that the distribution of $CO_2$ fluxes between sea ice and the atmosphere alternate between negative and positive fluxes, and that $CO_2$ fluxes close to zero are the most frequent and widespread, occurring consistently across seasons in both the Arctic and Southern Ocean (Fig. 2).

In both polar oceans, sea ice exhibits a pronounced seasonality in the direction of air–ice $CO_2$ fluxes (Fig. 2c). Sea ice tends to release $CO_2$ during fall and winter, while acting as a sink and taking up atmospheric $CO_2$ in summer, a pattern consistently highlighted in previous studies. During freezing, brine within the ice becomes highly supersaturated in $CO_2$, essentially due to the solute concentration effect as water is removed to the solid phase[19,20,23,43], driving a net $CO_2$ release to the atmosphere (as well as to the underlying water). Calcium carbonate precipitation and microbial respiration are secondary processes that could potentially also increase brine $CO_2$ partial pressure ($pCO_2$) in winter. In contrast, during summer melting processes dilute brine, reducing $pCO_2$, which results in marked undersaturation relative to the atmosphere, favouring $CO_2$ uptake[13,15,16,18,54]. Temporary sea-ice surface features further modulate this seasonal cycle. For example, frost flowers, which typically form on thin ice or leads during fall and winter[20,55], systematically act as sources of $CO_2$ (median +1.7 mmol $m^{-2}$ $day^{-1}$), while melt ponds which form throughout late spring and summer consistently act as sinks, because of their low salinities, coupled with moderate primary production (median –1.0 mmol $m^{-2}$ $day^{-1}$; Fig. 2b). Finally, slush exposed to the atmosphere after snow removal and resulting from flooding in the Southern Ocean acts as a sink for, more often than a source of atmospheric $CO_2$[54].

Fluxes measured over snow-covered sea ice show the least variability, with fluxes consistently close to zero (median (IQR) 0.00 (–0.03,+0.03) mmol $m^{-2}$ $day^{-1}$), suggesting that snow over sea ice limits gas exchange (Fig. 2b), although fluxes are dependent on snow properties and wind (i.e., wind pumping)[20,61]**.** In the Arctic, MYI has long been considered impermeable to gas exchange during winter, owing to the low brine volume at the ice-atmosphere interface resulting from both its low salinity and cold temperatures. However, data from the MOSAiC expedition revealed small but measurable fluxes over MYI even during the winter months[57].

### 2.3. The significance of the sea-ice $CO_2$ source and sink

To establish air-sea exchange budgets for the Arctic and Southern Oceans, we first derived representative daily $CO_2$ fluxes for each month in each ocean. In the Arctic, we further separated the contributions from FYI (i.e, total ice area minus MYI), summer ice (i.e., total ice area excluding melt ponds), MYI defined by the September sea-ice area, and melt ponds. In the Arctic, these representative fluxes were then extrapolated to the corresponding monthly areas of FYI (October-April), MYI, summer ice, and melt ponds (see Method, Fig. 6). In the Southern Ocean, the representative fluxes were simply extrapolated to the total sea-ice area. Summing the resulting monthly fluxes provided estimates of the net $CO_2$ drawdown into (or release from) the sea ice for both the Southern and Arctic Oceans (Fig. 3 & 4, Supplementary Table S1). The methodology used for the extrapolation and budget calculations is detailed in the Method section. The monthly and yearly net sea-ice $CO_2$ drawdown (or release) is further

compared with the net open water $CO_2$ drawdown (or release) of the Arctic Ocean, as defined by the RECCAP2 Arctic domain[49], and the Southern Ocean sea-ice zone (SIZ), as defined by the ice biome RECCAP2 definition[62] (Fig. 3 & 4, Supplementary Fig. S1, Table S3). The methodology used to establish the open-water $CO_2$ flux budgets is detailed in the Supplementary Material (sections S2.1 and S2.2).

### 2.3.1. In the Southern Ocean

Air–ice $CO_2$ fluxes are consistently an order of magnitude lower than air–sea fluxes (Fig. 3a, Supplementary Tables S1 and S3). In winter (July–September), median air–ice fluxes range from +0.1 to +0.2 mmol $m^{-2}$ $day^{-1}$, making sea ice a net source releasing 2 Tg C. During the same period, the open waters of the Southern Ocean sea-ice zone (SIZ) release close to ten times more $CO_2$ (22 Tg C) than the sea ice itself. In spring (October–December), air–ice fluxes shift towards negative values (median fluxes of 0.0 to –0.1 mmol $m^{-2}$ $day^{-1}$), and sea ice acts as a sink, absorbing 1 Tg C. Similarly, the open waters of the Southern Ocean SIZ also evolve

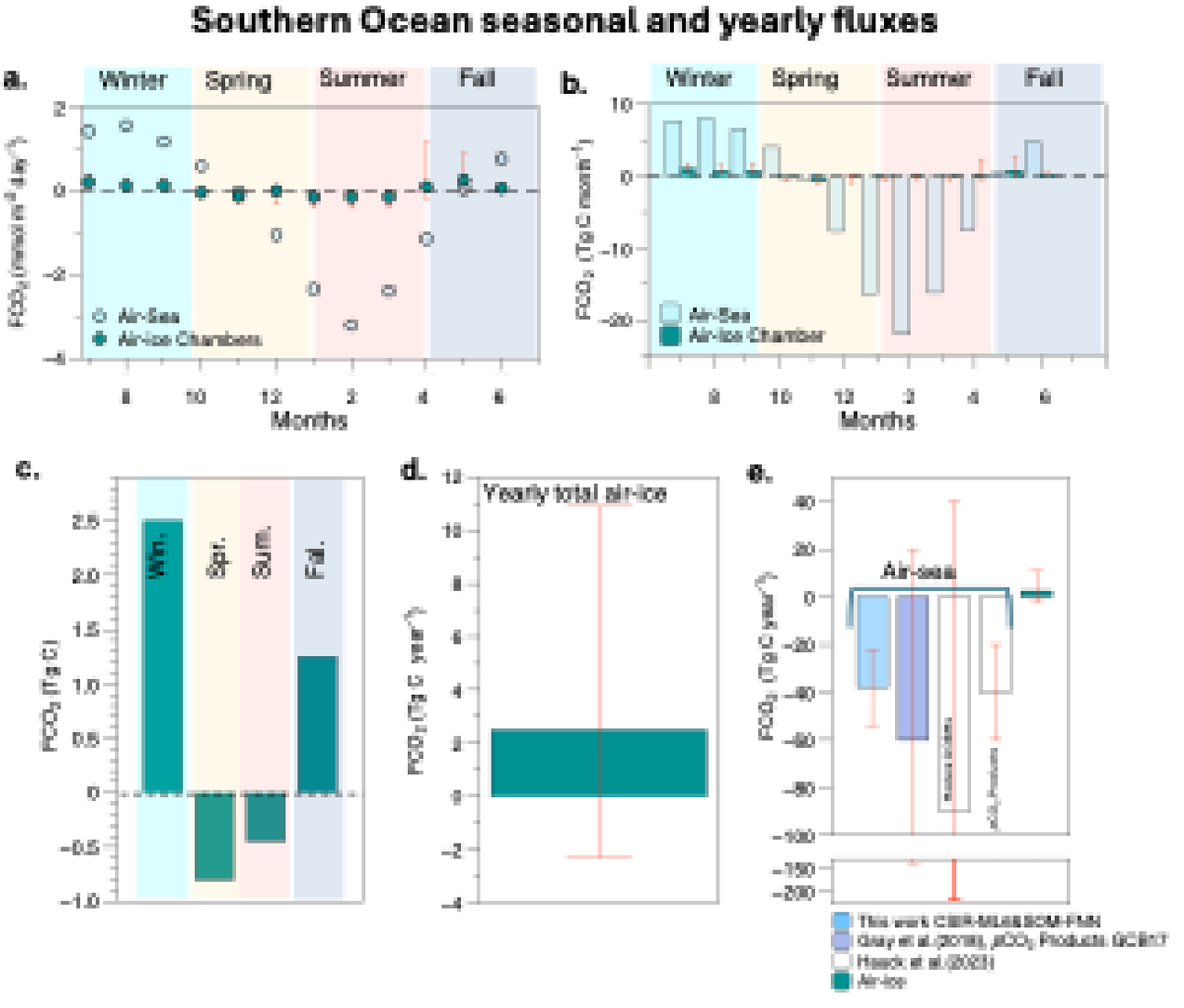

toward a sink, taking up about 4 Tg C over the three-month period. This sink behaviour continues into summer (January–March), with median air-ice fluxes around –0.1 mmol $m^{-2}$ $day^{-1}$ in January, contributing to a small additional uptake of 0.5 Tg C, assuming that the measurements conducted in January are representative of the entire summer season. With the minimum sea-ice extent during these months, the open waters of the Southern Ocean SIZ act as a strong sink, taking up 54 Tg C. By fall (April–June), sea ice switches back to a source, showing the highest median air-ice fluxes of the seasonal cycle and releasing about 1 Tg C. During the fall, the open waters of the Southern Ocean SIZ transition from a substantial sink to a source, with a net drawdown of 2 Tg C from April through June (Table S2).

**Fig. 3 Southern Ocean seasonal and yearly fluxes.** (a) Seasonal evolution of air-sea and air-ice $CO_2$ fluxes in mmol $m^{-2}$ $day^{-1}$ in the Southern Ocean. Air-sea fluxes are from an assembly of $pCO_2$ products (supplemental material, Section S2.1, Table S3). Air-ice chamber fluxes are the medians derived from the database (see Method and Supplementary Table S1). (b) Monthly $CO_2$ flux in Tg per month for the total sea-ice and ocean areas (see Method and Supplementary Table S1). (c) Net seasonal sea-ice $CO_2$ exchange in Tg. (d and e) sea-ice net annual $CO_2$ fluxes in Tg per year compared to air–sea net yearly $CO_2$ fluxes from this work, Gray et al.[47] and Hauck et al.[48]. Error bars in a, b, d and e for sea ice show the 25th–75th percentiles (IQR) around each median estimate.

Most of the winter air–ice $CO_2$ emissions in the Southern Ocean are offset by spring and summer uptake, resulting in sea ice being a small net source of about 2.5 (IQR: –2.3,+10.9) Tg C per year. This net release of carbon is quite low compared to recent assessments of air–sea $CO_2$ fluxes of the Southern Ocean SIZ (Fig. 3e). Using available $pCO_2$ products extrapolated over the open water areas we estimate an annual ocean uptake of –38.1 Tg C $yr^{-1}$ (Supplementary, section S1.1, Table S3), similar to recent estimates based on other $pCO_2$ assemblages reporting annual uptake ranging from –40 to –60 Tg C $yr^{-1}$ in the Southern Ocean SIZ (Fig. 3e). In contrast, ESMs predict a stronger uptake of around –90 Tg C $yr^{-1}$[48]. Within this context, the role of sea ice is minor, accounting for less than 5% of the Southern Ocean SIZ's annual ocean uptake.

### 2.3.2. In the Arctic Ocean

Similar to the Southern Ocean, Arctic median air–ice $CO_2$ fluxes for each month derived from the database, are one to two orders of magnitude lower than air–sea fluxes, except in February (Fig. 4a, Supplementary Tables S1, S3). In winter (January–March), median air–ice fluxes range from +0.1 to +1.4 mmol $m^{-2}$ $day^{-1}$, indicating that sea ice acts as a source of $CO_2$, releasing about 6 Tg C to the atmosphere. The MYI air-ice fluxes (0.1 mmol $m^{-2}$ $day^{-1}$) contribute less than 10% of this winter release (0.3 Tg C; Fig. 4c). Over the same period, the open water fraction acts as a net sink, taking up approximately 19 Tg C (Fig. 4b). During spring (April–June), air–ice fluxes decrease to become slightly negative by June (–0.3 mmol $m^{-2}$ $day^{-1}$). Sea ice shifts from a weak source to a weak sink through the spring, taking up less than 1 Tg C, while open water continues to absorb around 21 Tg C. In summer (July–September), the ice is a consistent sink, with median fluxes up to –0.8 mmol $m^{-2}$ $day^{-1}$, while median melt

pond fluxes are –1.0 mmol $m^{-2}$ $day^{-1}$. Overall, in summer, sea ice takes up 3 Tg C, with melt ponds contributing more than 55% of this sea-ice-associated summer sink (Fig. 4c). Meanwhile, the open water fraction absorbs approximately 36 Tg C. Finally, in fall (October–December), the ice again begins releasing $CO_2$, with median positive fluxes ranging from 0.1 to 0.2 mmol $m^{-2}$ $day^{-1}$. Throughout fall, sea ice shifts back to being a minor net source, releasing about 1 Tg C, while the open water continues to act as a strong sink, taking up around 30 Tg C.

On an annual basis, most of the winter $CO_2$ emissions from sea ice are offset by spring and summer uptake, resulting in Arctic sea ice acting as a small net source of about 3.8 (IQR: –7.8, +17.0) Tg C $yr^{-1}$ (Fig. 4d). In contrast, the open water of the Arctic Ocean consistently functions as a strong sink, with a cumulative annual uptake of approximately 100 Tg C $yr^{-1}$

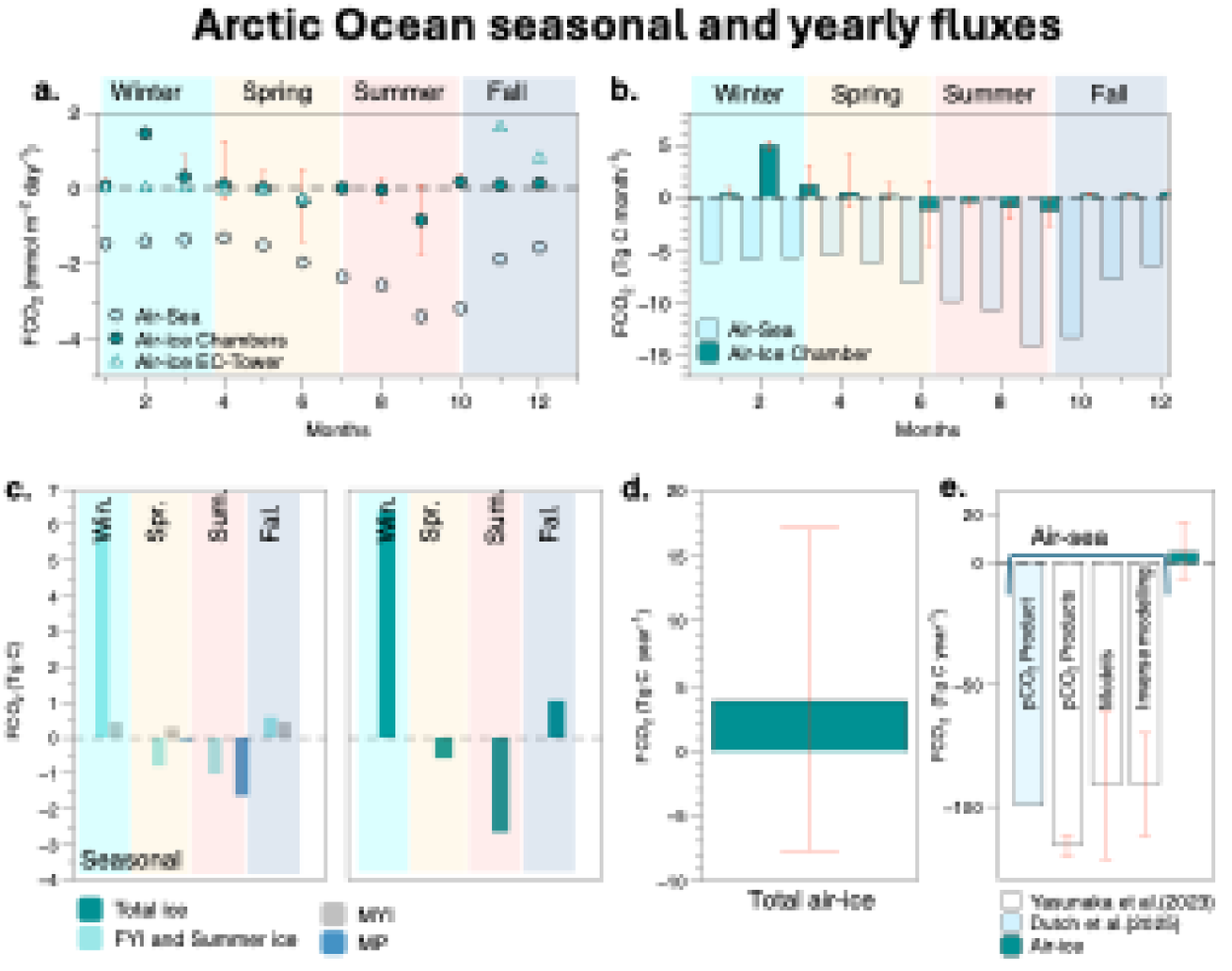


(Fig. 4e; Supplementary section S2.2). While winter ice-atmosphere fluxes can at times compete with concurrent ocean uptake, making sea ice seasonally relevant for basin-scale estimates, its annual contribution remains minor, accounting for less than 5% of the yearly ocean uptake.

**Fig. 4 Arctic Ocean seasonal and yearly fluxes.** (a) Seasonal evolution of air-sea and air-ice $CO_2$ fluxes in mmol $m^{-2}$ $day^{-1}$ for the Arctic Ocean. Air-sea fluxes are from Dutch et al.[46], air-ice chamber fluxes are median values derived from our database (see Method, and

Supplementary Tables S1, S3), and air-ice EC-Tower fluxes are measurements from Butterworth et al.[64] (b) Monthly $CO_2$ fluxes in Tg per month for the total sea-ice and ocean areas (see Method, and Supplementary section S2.2, Table S1, S3 ). (c) Seasonal net $CO_2$ exchange in Tg for the different ice types and for the total sea-ice area as the sum of the contributions of the different ice types. (d) and (e) are sea-ice net annual $CO_2$ fluxes in Tg per year (d) compared to (e) air–sea net yearly $CO_2$ fluxes from Dutch et al.[46] and Yasunuaka et al.[49]. Error bars in a, b, d, and e for sea ice show the 25th–75th percentiles (IQR) around each median estimate.

### 2.4. Limitations and uncertainties in the role of the sea ice in the carbon budget

It is essential to acknowledge that chamber-based flux measurements are susceptible to several biases [41]. They inherently disturb the surface environment, isolating it from natural atmospheric conditions and changing the radiation balance and temperature profile. Most importantly, they block the wind, dampening the turbulence and wind pumping that are some of the main drivers of gas fluxes [63], thereby measuring only diffusive fluxes. Thus, in general, chamber-based flux measurements should be considered a minimum estimate of natural environmental fluxes. In addition, two of the most important limitations of chamber-based flux measurements are their restricted spatial coverage and their inability to provide continuous measurements. The lack of continuous data is especially critical in early spring, when sea ice undergoes strong diurnal cycles of $CO_2$ fluxes: daytime warming above 0 °C can drive $CO_2$ uptake, while nighttime freezing often results in outgassing[13,64]. Depending on the timing of deployment, chambers may therefore capture either net uptake or net release, introducing substantial uncertainty into the measurements. Despite these limitations, the overall mean ($+0.09 \pm 1.28$ mmol $m^{-2}$ $day^{-1}$), median (0.00, IQR: 0.00, +0.17 mol $m^{-2}$ $day^{-1}$), and seasonal pattern of our Arctic dataset align well with recent continuous $CO_2$ flux measurements over Arctic sea ice[64]. That study reported eddy covariance (EC) fluxes over landfast sea ice near Cambridge Bay, Canada, from autumn freeze-up through spring breakup (Fig. 4a). The EC and chamber datasets agree particularly well in spring. Spring is the most extensively sampled season, with 3,499 measurements collected across the Arctic between April and June, thereby partially reducing spatial and diurnal biases in our database.

Nonetheless, some discrepancies are evident between the EC and chamber datasets, particularly in winter and fall. Strong outgassing during the initial ice growth phase has been measured by EC[64], but chamber measurements are rarely obtained over thin ice, explaining some of the discrepancy in the fall season (Fig. 4a). During spring there is better agreement between the methods. Due to logistical constraints, Butterworth et al.[64] obtained limited measurements during winter but generally recorded negligible fluxes when air temperatures were below –20°C, suggesting that at extremely low temperatures sea ice becomes impermeable to gas exchange. Delille et al.[16] similarly suggested that fluxes stop below –8°C, while other studies have proposed that sea ice becomes impermeable once brine volume

fraction drops below 5%[9]. However, our extensive dataset shows that gas exchange at the air–ice interface cannot be explained solely by temperature or brine volume thresholds. Fluxes close to 0.00 mmol $m^{-2}$ $day^{-1}$ occur throughout the year in both polar oceans, independent of the sea-ice temperature, and significant positive fluxes have been observed even at temperatures below –15°C (Fig. 5). This indicates that sea-ice permeability and gas exchange are not solely controlled by temperature. For instance, the formation of an impermeable surface layer due to snow melt and refreezing (superimposed ice) can greatly reduce air–ice gas exchange, while the presence of brine skim and wetted snow, as well as the development of micro-cracks from rapid freezing under very cold conditions, can enhance the exchange[13,61]. These interfacial processes occur at various spatial and temporal scales, making it challenging to establish a simple parameterisation of air–ice exchange based solely on temperature or brine volume fraction. Nevertheless, temperature appears to strongly influence the direction of the fluxes: above –4 °C, over 90 % of the fluxes indicate uptake by the sea ice (Fig. 5), whereas fluxes observed at the lowest temperatures indicate almost exclusively $CO_2$ release to the atmosphere. This behaviour is consistent with the well-established influence of sea-ice temperature on internal $pCO_2$, which in turn determines the $pCO_2$ gradient between the ice and the overlying atmosphere[23].

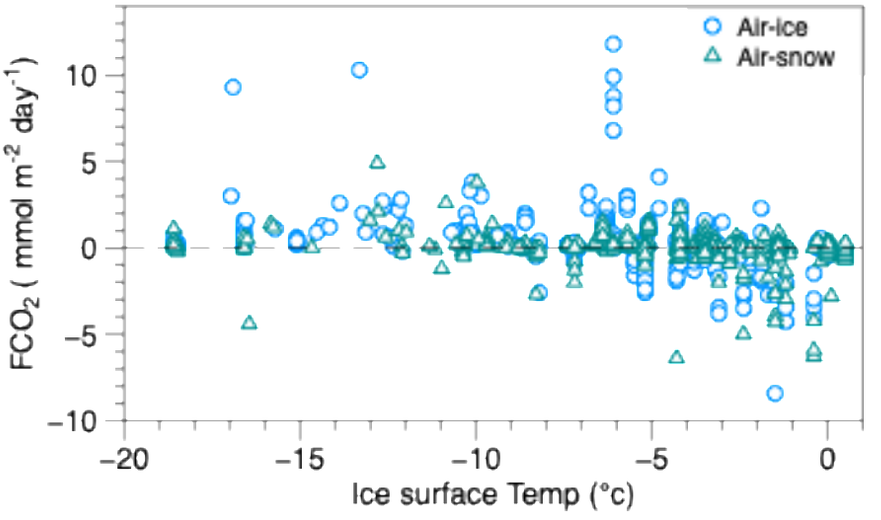


**Fig. 5 Relationship between air-ice $CO_2$ fluxes and ice surface temperature.** $FCO_2$ in mmol $m^2$ $day^{-1}$ and ice surface temperature from both polar oceans. This is a subset of the database for which ice surface temperatures were available.

Another key factor controlling flux magnitudes is ice thickness. Young, thin ice has been shown to release much more $CO_2$ than thicker, more mature ice [20,52,64]. Thin, newly formed sea ice is highly permeable, allowing efficient outgassing from the $CO_2$-enriched brines to the atmosphere. In contrast, thicker, mature ice is less permeable, limiting brine connectivity and thereby reducing air–ice $CO_2$ fluxes. The largest discrepancy between our chamber-based dataset and the EC data from Butterworth et al.[64] occurs in the fall (Fig. 4a). Butterworth et al.[64] reported positive fluxes exceeding +1 mmol $m^{-2}$ $day^{-1}$ and estimated that sea ice could release 7-10 Tg C during October–December across the Arctic Ocean, which is markedly higher than the 1 Tg C derived from our chamber database (supplementary table S1).

Butterworth et al.[64] attributed these large fluxes to outgassing during the initial freezing of thin ice (conditions under which chamber deployments are particularly difficult), which declines as the ice thickens by December. In the Southern Ocean, although fall exhibits the highest fluxes of the year (Fig. 2c), the median flux during these months remains low and does not exceed 1 mmol $m^{-2}$ $day^{-1}$ (Fig. 3a), even though the upper quartile reaches the highest values observed annually. Such large fluxes from newly forming ice are typically short-lived. These transient events are difficult to capture at the scale of the entire Arctic and Southern Oceans, and our dataset likely missed such episodic high fluxes during fall, particularly because this season is under-sampled (i.e., only 51 data points from two field campaigns in the Arctic and 40 data points from two campaigns for the Southern Ocean). This makes large-scale extrapolation challenging, especially during transitional periods such as the fall, when spatial heterogeneity is high. For example, in December, the high Arctic already experiences deep winter conditions with thick ice and minimal fluxes, whereas in the lower latitude Arctic, sea ice may still be forming and actively outgassing. Similarly, the chamber database compiled here includes measurements over thin, growing sea ice from leads during February through May in the Arctic with fluxes typically exceeding +1 mmol $m^{-2}$ $day^{-1}$. As February is also among the least sampled months in the Arctic, the elevated fluxes recorded over thin ice disproportionately influence the database (Fig. 4a) and are unlikely to reflect the broader sea-ice conditions prevailing across the Arctic at that time. The current budget may therefore underestimate fall fluxes in both polar oceans while overestimating winter fluxes. Therefore, to reduce the impact of this spatial and seasonal heterogeneity on estimates of polar carbon budgets, increased sampling is needed during fall and winter and across both polar regions.

Overall, the scarcity of data in time and space, combined with the high variability of recorded fluxes, leads to substantial uncertainties in the sea-ice carbon budget. For the Arctic Ocean, our estimates range from –7 to +17 Tg C $yr^{-1}$, with a median value of +4 Tg C $yr^{-1}$ (Supplementary Table S1). In the Southern Ocean, our estimate of sea-ice carbon exchange spans from –2 to +11 Tg C $yr^{-1}$, with a median value of +2 Tg C $yr^{-1}$. While these are the first basin-scale estimates of air-ice $CO_2$ fluxes in the Arctic and Southern Oceans, these numbers are likely to evolve rapidly given the climate change-related changes in the ice cover in both oceans [65,66]. The primary consequence of MYI loss is an increase in the open-water fraction during summer. This transition replaces relatively small air–ice fluxes with stronger air–sea fluxes. In winter, MYI is largely replaced by FYI, indicating enhanced sea-ice formation and potentially increased outgassing.

### 2.5. Key findings

This study provides the first basin-scale synthesis of air–ice $CO_2$ fluxes in both the Arctic and Southern oceans, based on more than 6,000 chamber measurements collected over two decades. Despite their spatial and temporal limitations, these data allow for the derivation of monthly and annual sea-ice carbon budgets and provide critical context for evaluating the role of sea ice in the polar ocean carbon budget.

Our results show that on an annual basis, sea ice acts as a small net source of $CO_2$, with median values of +4 Tg C $yr^{-1}$ in the Arctic and +2 Tg C $yr^{-1}$ in the Southern Ocean. In contrast, the oceanic uptake is estimated at up to nearly 100 Tg C $yr^{-1}$ in each ocean[46–49]. These results

refine previous estimates, such as those of Delille et al.[16], who, based on a limited subset of the full database we have compiled here, suggested that sea ice could take up as much as 29 Tg C during spring (October–November) in the Southern Ocean. Our synthesis, grounded in a much broader dataset, estimated spring uptake around 1 Tg C, showing that such large seasonal fluxes are unlikely. More generally, while earlier studies hypothesised that even small air–ice $CO_2$ fluxes could accumulate to significant values due to the vast extent of polar sea ice and therefore recommended including sea-ice contributions in carbon budget assessments, our analysis suggests that the net annual role of sea ice is minor at the basin scale. From a modelling perspective, while the explicit inclusion of air–ice $CO_2$ exchange in Earth system models has been recommended, the current lack of reliable parameterisations and the large uncertainties associated with flux estimates make such inclusion premature. Given that winter and summer fluxes offset each other and are 1 to 2 orders of magnitude smaller than air-sea exchange, treating sea-ice fluxes as negligible at the basin scale may remain the most defensible assumption, at least for broad-scale carbon budget estimates such as those carried out by Earth system models. On the other hand, exchange between the atmosphere and sea ice could be relevant for high-resolution regional models investigating processes occurring on shorter time scales.

These results highlight that sea ice functions as a permeable, rather than an absolute, barrier to gas exchange, allowing intermittent yet measurable exchanges with the atmosphere. While the overall role of sea ice in the global carbon budget is minor, the same cannot be assumed for other climatically relevant trace gases, such as dimethyl sulfide, volatile organic carbons, or halogens, for which the ocean is not the primary reservoir. For these chemical species, even modest air–ice fluxes could significantly influence atmospheric concentrations, especially when seasonal emissions and drawdowns do not fully offset each other.

Nonetheless, important uncertainties remain. The strong variability of fluxes, the scarcity of winter and fall data, and the inability of chambers to capture continuous diurnal cycles or episodic events all contribute to wide uncertainty ranges. Also, because of their design, which dampens turbulence, chambers tend to underestimate fluxes. Transient outgassing from newly forming thin ice during fall and winter may be underrepresented, potentially leading to an underestimation of seasonal fluxes. Moreover, surface processes such as slush, brine skim and frost-flower formation, and micro-cracking, which all exert significant control on sea-ice permeability and $CO_2$ exchange, remain difficult to quantify and integrate across space and time at large scales.

## 3. Method

### 3.1. Air-ice first-order budget estimation

To establish the budget, we first use measurements from the database to derive average daily $CO_2$ fluxes for each month for each ocean. These fluxes are then extrapolated to the monthly ice area. Summing those monthly fluxes provides estimates of net $CO_2$ drawdown into (or release from) the sea ice of the Southern and Arctic Oceans.

In the Arctic, the compiled database and satellite products allow us to distinguish the contributions of first-year ice (FYI), multi-year ice (MYI), and melt ponds (MP). Differentiating between these surface types is essential because they exhibit distinct physical and biogeochemical properties that strongly influence air-ice $CO_2$ exchange. Under cold conditions, MYI generally has lower permeability and reduced brine volume than the thinner,

more saline FYI; however, in summer, FYI can no longer be discriminated from MYI, as surface warming and melting make MYI as permeable as FYI. Therefore, in winter, spring, and fall, we derived monthly FYI fluxes from FYI data, whereas in summer, monthly fluxes are based on measurements from both FYI and MYI. In addition, the summer months include melt pond fluxes, as melt ponds form in late spring and persist through summer, substantially enhancing gas exchange by exposing areas of liquid water on the ice surface.

In contrast, in the Southern Ocean, sea ice is predominantly first-year ice with limited melt pond development. Although features such as polynyas and slush layers over flooded ice can be spatially significant, the compiled database and available satellite products do not allow these to be consistently distinguished. Therefore, monthly fluxes were extrapolated to the total sea-ice area without further subdivision.

#### 3.1.1. Data selection – Panel 1 of Figure 6

In the Arctic, to compute the daily fluxes for FYI during winter months, we excluded fluxes over bare sea ice and frost flowers from our analysis (Fig. 6a). In winter, sea ice is nearly always covered by snow, and including fluxes over bare sea ice from which the snow had likely been removed for the measurement would not accurately represent the surface natural state. Frost flower fluxes are also not representative of typical fluxes and are not suited for large-scale extrapolation, given that they are short-lived phenomena of limited spatial extent that occur sporadically under very specific conditions (e.g., thin ice, extreme cold weather[67]). For the spring and summer months, we included data from snow-covered and bare sea ice, as snow cover drastically decreases during this period. In the fall, we included both fluxes from snow-covered and bare sea ice, since new ice might not yet have snow on its surface.

In the Southern Ocean, we included only measurements over snow. Slush is spatially relevant in the Southern Ocean, given the extent of flooded sea ice, but most slush flux measurements were obtained after artificially removing snow and deliberately exposing the slush to the atmosphere.

#### 3.1.2. Statistical treatment –Panel 2 of Figure 6

Since flux values do not follow a normal distribution (Shapiro-Wilk test, $p<0.05$), the representative daily $CO_2$ flux for each month in each ocean is based on the median and interquartile range rather than the mean and standard deviation. Some campaigns deployed autonomous $CO_2$ chambers capable of producing up to 48 measurements over 25 hours, while others used manual chambers, limiting the number of measurements to 3 per day. To give each survey representing a single location in the ocean the same relative importance and avoid statistical bias, the monthly data were first binned by survey, and monthly median (IQR) fluxes were derived from the binned data (Fig. 6c-g).

In the Arctic, we also derived a representative flux for MYI in winter, fall, and spring. Since the database lacks systematic MYI measurements for each month, it is not possible to derive monthly MYI fluxes. Instead, we compute a single representative daily $CO_2$ flux based on the median (IQR) of the 40 MYI measurements available throughout the winter (Fig. 6b). Similarly, we derived a single representative summer melt pond (MP) flux based on the 25 measurements available in the database (Fig. 6b).

#### 3.1.3. Data extrapolation –Panel 3 of Figure 6

In winter, fall and spring, monthly representative fluxes for FYI were extrapolated to the FYI, defined as the total ice area minus the MYI area and representative MYI flux is applied to the monthly MYI area, defined as the ice area in September (Fig. 6h-j, Supplementary Tables S1 and S2). The mean monthly sea-ice area was derived for the years 2000-2023 from EUMETSAT OSI SAF, Global sea-ice concentration interim climate data record (SSMIS, v3.0,

2022)[68]. In summer, FYI and MYI are no longer distinguished; monthly representative fluxes for ice were extrapolated to what we called summer ice, defined as the total ice area excluding melt pond area (Fig. 6h-j, Supplementary Table S2). Melt pond fluxes were applied to the monthly melt pond area. The mean monthly melt pond area was extracted from the improved Melt Pond Detector 2 (MPD2) Sentinel-3 data for the years 2017 to 2023[69]. Total air-ice $FCO_2$ is the sum of the monthly contributions of each ice type (Fig. 6k).

For the Southern Ocean, the daily representative fluxes for each month were applied to the sea-ice area for that month. Since there were no data for the summer months (February and March), we applied the January fluxes to those months as well. Similarly, there were no data in the winter month of August, so we applied the September fluxes to August.

Finally, the yearly budget is derived by summing the contributions for each month (Fig. 6l, Supplementary Tables S1 and S3).

## 1. Data selection for the Arctic

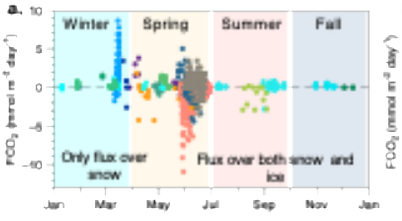


Filled circle color represents a survey.

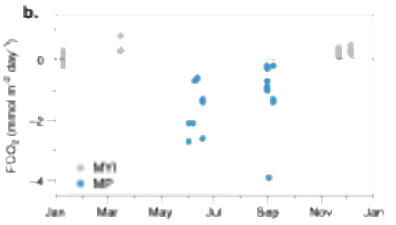


**1.1.** From the 4719 Arctic measurements, 4117 fluxes from snow and ice, 25 fluxes over melt ponds (MP), and 40 measurements from multi-year ice (MYI) are included in the statistical analysis to establish the budget.

## 2. Statistical treatment

**2.1.** Binning data per survey for each month

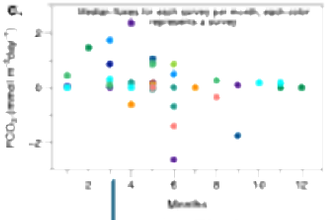


**2.2.** Monthly Median fluxes based on the binned data

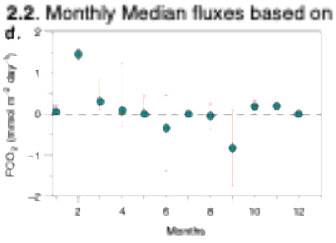


Binning example for March

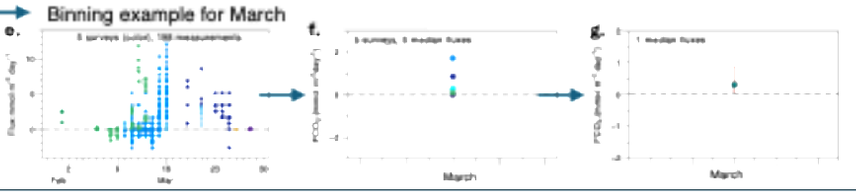


## 3. Data extrapolation for monthly Budget

**3.1.** Convert $FCO_2$ in mmol $m^{-2}$ $d^{-1}$ to $FCO_2$ in g C $km^{-2}$ $month^{-1}$

**3.2.** Extrapolate the carbon fluxes to sea ice area to obtain C fluxes in Tg $month^{-1}$

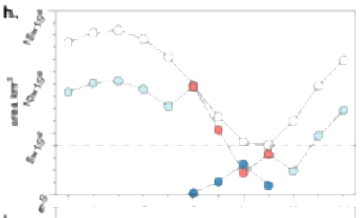


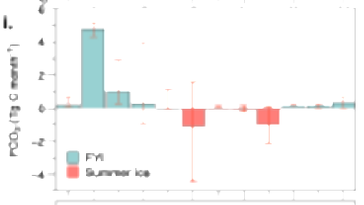


- In winter and fall, monthly fluxes are applied to the FYI area. FYI area is defined as the total ice area minus the MYI area
- From May to September, the monthly fluxes are extrapolated to summer sea ice area, defined as is the total sea ice area minus the melt pond area.

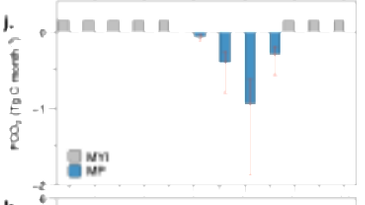


- The MYI ice contribution is based on the median flux of 40 measurements applied to the monthly MYI area. MYI ice is defined as the ice area of September.
- The melt-pond contribution is based on the median flux of 25 measurements applied the monthly melt pond area.

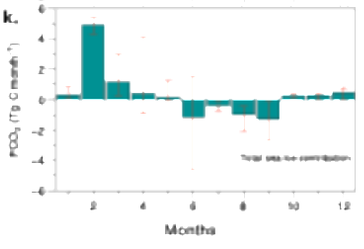


- Total sea-ice contribution: addition of contribution of FYI, Summer ice, MYI and melt pond .

**3.3.** Yearly budget: summing the contribution of each month

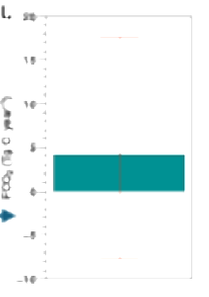

**Figure 6. Scheme of the methodology** used to establish the monthly and yearly budget for the Arctic Ocean. Panel (a-b) are raw air–ice $CO_2$ fluxes in mmol $m^{-2}$ $day^{-1}$, and panel (c-g) shows median air–ice $CO_2$ fluxes in mmol $m^{-2}$ $day^{-1}$. Panel (h) is the sea ice extent area in $km^2$. Panel (i-j) are air–ice $CO_2$ fluxes in Tg C $month^{-1}$ for first-year ice (FYI), summer ice, multi-year ice (MYI) and melt pond (MP). Panel (g) shows the total monthly air–ice $CO_2$ fluxes in Tg C $month^{-1}$ and panel (l) shows the yearly budget of air–ice $CO_2$ fluxes in Tg C $year^{-1}$. Error bars in panels (d), (g), (i), (j), (k), and (l) show the 25th–75th percentile around each median estimate.

**Acknowledgements**

We particularly wish to thank all the scientists who contributed their data to the compiled database; all of those measurements were hard work, and many of them were made under extremely difficult conditions. We also thank Gunnar Spreen and Hannah Niehaus for their help in determining the melt pond area. This paper is a product of the Biogeochemical Exchange Processes at Sea-Ice Interfaces (BEPSII) research community, which is jointly sponsored by the Scientific Committee on Antarctic Research (SCAR), the WCRP core program Climate and Cryosphere (CliC), and the Surface Ocean-Lower Atmosphere Study (SOLAS, via NSF grants #OCE-1840868, 2140395, and 2513154 to SCOR).

**Funding**

This paper is a contribution of SCOR Working Group 152, Measuring Essential Climate Variables in Sea Ice (ECV-Ice). This work was supported by the F.R.S-FNRS (grants 2.4649.07, 2.4584.09, j.0161.13, T.0268.16, J.0262.17, J.0051.20) and the Belgian Science Policy (BELCANTO III, SD/CA/03Aigsouth SD/CA/05A and OCeANIC OBL/12/C63). It was also part of the GreenFeedBack RIA (Greenhouse gas fluxes and earth system feedback) funded by the European Union's HORIZON research and innovation program under grant agreement No. 101056921 and UK Research and Innovation under grant agreement #10040851. Views and opinions expressed are, however, those of the authors only and do not necessarily reflect those of the European Union or CINEA. Neither the European Union nor the granting authority can be held responsible for them. OC and BD are post-doc and research associate, respectively, at the F.R.S.-FNRS. SM acknowledges support from the Research Council of Norway (I-CRYME project 11993, DIAMOND project 352217, and iC3 Center of Excellence 332635 project) and the EU (WOBEC 350906 Biodiversa project), DN was supported by the Japan Society for the Promotion of Science (grant 25H00679, 24H02341, 24H04715), JST CREST, Japan, Grant Number JPMJCR23J5, the Arctic Challenge for Sustainability II (JPMXD1420318865). BE acknowledges support from the Natural Sciences and Engineering Research Council of Canada (NSERC) Discovery Grant program.

**Data availability.**

The dataset of air-ice $CO_2$ fluxes based on chamber measurements supporting this study is publicly available via the Zenodo data repository (DOI **10.5281/zenodo. 19233335)**. This repository contains the raw data necessary to reproduce the air–ice $CO_2$ fluxes presented in

Figures 1, 2, 3, 4, and 5. The data used to reproduce the air–sea $CO_2$ exchange based on the Arctic SOM-FFN $pCO_2$ product (Fi. 4a) are available at: https://zenodo.org/records/15056124. The analysis code and the resulting data from calculating the ensemble mean CO2 fluxes in the Southern Ocean sea ice zone (RECCAP2) (Fig. 3A) using both CSIR-ML6 (v2019a) pCO2 product (Gregor et al., 2019) and MPI-SOMFFN (v2023) pCO2 product (Landschutzer et al., 2016) are now available on Zenodo with the DOI: https://doi.org/10.5281/zenodo.19360167. Air-ice $CO_2$ fluxes from Butterworth et al., 2025, used in Fig 4a have been published on the Zenodo data repository. They can be found at the following link: https://doi.org/10.5281/zenodo.15191010 (Else and Butterworth, 2025).

**The author's contribution.**

O. Crabeck, D. Nomura, and B. Delille contributed to the acquisition of data and the compilation of the database. O. Crabeck proceeded to analyse air-ice $CO_2$ fluxes and derive budgets. L.M. Djeutchouang and V.R. Dutch contributed to the analysis of air-sea $CO_2$ Fluxes. O. Crabeck drafted the article. D. Nomura, S. Moreau, B.G.T. Else, L.A. Miller, and B. Delille revised and approved the submitted version for publication.

**Competing interests**

The authors declare no competing interests.

**Figures captions**

**Fig. 1 Spatial and temporal coverage of the data compilation.** (a) Seasonal representation of the dataset, percentage (%) of the measurements in each ocean collected during each month of the year. (b) Spatial distribution of the dataset. The number following each location references a field campaign listed in Table 1.

**Fig. 2: Key characteristics of the data compilation.** (a) Histogram of air–ice $CO_2$ fluxes in mmol $m^{-2}$ $day^{-1}$ , and (b) interquartile (IQ) box plot of air–ice $CO_2$ fluxes in mmol $m^{-2}$ $day^{-1}$ per ice type; the number in brackets is the number of measurements for each category (SO = Southern Ocean, AO = Arctic Ocean, FF = frost flowers, MP = melt pond). The centre line is the median, the limits of the box are the first (Q1) and third quartile (Q3), the whiskers are drawn to the smallest/largest non-outlier. Outliers are defined as either Q1-1.5 IQR or Q3+1.5 IQR. (c) Seasonal distribution of air–ice $CO_2$ fluxes in mmol $m^{-2}$ $day^{-1}$ for the Arctic and Southern Oceans. Positive fluxes indicate $CO_2$ transport to the atmosphere; negative fluxes indicate $CO_2$ uptake by the sea ice.

**Fig. 3 Southern Ocean seasonal and yearly fluxes.** (a) Seasonal evolution of air-sea and air-ice $CO_2$ fluxes in mmol $m^{-2}$ $day^{-1}$ in the Southern Ocean. Air-sea fluxes are from an assembly of $pCO_2$ products (supplemental material, Section S2.1, Table S3). Air-ice chamber fluxes are the medians derived from the database (see Method and Supplementary Table S1). (b) Monthly $CO_2$ flux in Tg per month for the total sea-ice and ocean areas (see Method and Supplementary Table S1). (c) Net seasonal sea-ice $CO_2$ exchange in Tg. (d and e) sea-ice net annual $CO_2$ fluxes in Tg per year compared to air–sea net yearly $CO_2$ fluxes from this work, Gray et al.[47] and

Hauck et al.[48]. Error bars in a, b, d and e for sea ice show the 25th–75th percentiles (IQR) around each median estimate.

**Fig. 4 Arctic Ocean seasonal and yearly fluxes.** (a) Seasonal evolution of air-sea and air-ice $CO_2$ fluxes in mmol $m^{-2}$ $day^{-1}$ for the Arctic Ocean. Air-sea fluxes are from Dutch et al.[46], air-ice chamber fluxes are median values derived from our database (see Method, and Supplementary Tables S1, S3), and air-ice EC-Tower fluxes are measurements from Butterworth et al.[64] (b) Monthly $CO_2$ fluxes in Tg per month for the total sea-ice and ocean areas (see Method, and Supplementary section S2.2, Table S1, S3 ). (c) Seasonal net $CO_2$ exchange in Tg for the different ice types and for the total sea-ice area as the sum of the contributions of the different ice types. (d) and (e) are sea-ice net annual $CO_2$ fluxes in Tg per year (d) compared to (e) air–sea net yearly $CO_2$ fluxes from Dutch et al.[46] and Yasunuaka et al.[49]. Error bars in a, b, d, and e for sea ice show the 25th–75th percentiles (IQR) around each median estimate.

**Fig. 5 Relationship between air-ice $CO_2$ fluxes and ice surface temperature.** $FCO_2$ in mmol $m^2$ $day^{-1}$ and ice surface temperature from both polar oceans. This is a subset of the database for which ice surface temperatures were available.

**Figure 6. Scheme of the methodology** used to establish the monthly and yearly budget for the Arctic Ocean. Panel (a-b) are raw air–ice $CO_2$ fluxes in mmol $m^{-2}$ $day^{-1}$, and panel (c-g) shows median air–ice $CO_2$ fluxes in mmol $m^{-2}$ $day^{-1}$. Panel (h) is the sea ice extent area in $km^2$. Panel (i-j) are air–ice $CO_2$ fluxes in Tg C $month^{-1}$ for first-year ice (FYI), summer ice, multi-year ice (MYI) and melt pond (MP). Panel (g) shows the total monthly air–ice $CO_2$ fluxes in Tg C $month^{-1}$ and panel (l) shows the yearly budget of air–ice $CO_2$ fluxes in Tg C $year^{-1}$. Error bars in panels (d), (g), (i), (j), (k), and (l) show the 25th–75th percentile around each median estimate.

## Table

**Table 1.** List of measurements present in the database

## References

1. Dieckmann, G. S. & Hellmer, H. H. The Importance of Sea Ice: An Overview. in *Sea Ice* 1–22 (Wiley-Blackwell, 2010). https://doi.org/10.1002/9781444317145.ch1
2. McClish, S. & Bushinsky, S. M. Majority of Southern Ocean Seasonal Sea Ice Zone Bloom Net Community Production Precedes Total Ice Retreat. *Geophysical Research Letters* **50**, e2023GL103459 (2023). https://doi.org/10.1029/2023GL103459
3. Vancoppenolle, M. et al. Role of sea ice in global biogeochemical cycles: Emerging views and challenges. *Quaternary Science Reviews* **79**, 207–230 (2013). https://doi.org/10.1016/j.quascirev.2013.04.011
4. Willis, M. D. et al. Polar oceans and sea ice in a changing climate. *Elementa: Science of the Anthropocene* **11**, 00056 (2023). https://doi.org/10.1525/elementa.2023.00056
5. Yager, P. L. et al. The Northeast Water Polynya as an atmospheric CO 2 sink: A seasonal rectification hypothesis. *Journal of Geophysical Research* **100**, 4389 (1995). https://doi.org/10.1029/94JC01962
6. Ito, T., Follows, M. J. & Boyle, E. A. Is AOU a good measure of respiration in the oceans? *Geophysical Research Letters* **31**, (2004). https://doi.org/10.1029/2004GL020900
7. Manizza, M. et al. A model of the Arctic Ocean carbon cycle. *Journal of Geophysical Research: Oceans* **116**, 1–19 (2011). https://doi.org/10.1029/2011JC006998
8. Cox, G. F. N. & Weeks, W. F. Equations for determining the gas and brine volumes in sea-ice samples. *Journal of Glaciology* **29**, 306–316 (1983). **https://doi.org/10.3189/S0022143000008364**
9. Golden, K. M., Ackley, S. F. & Lytle, V. I. The percolation phase transition in sea ice. *Science* **282**, 2238–2241 (1998). https://doi.org/10.1126/science.282.5397.2238
10. Gosink, T. A., Pearson, J. G. & Kelley, J. J. Gas movement through sea ice. *Nature* **263**, 41–42 (1976). https://doi.org/10.1038/263041a0
11. Matsuo, S. & Miyake, Y. Gas composition in ice samples from Antarctica. *Journal of Geophysical Research* **71**, 5235–5241 (1966). https://doi.org/10.1029/JZ071i022p05235
12. Weeks, W. F. & Ackley, S. F. The Growth, structure and properties of sea ice. in *The Geophysics of Sea Ice* 9–164 (Springer US, London, 1986).
13. Van der Linden, F. C. et al. Sea Ice CO2 Dynamics Across Seasons: Impact of Processes at the Interfaces. *Journal of Geophysical Research: Oceans* **125**, (2020). https://doi.org/10.1029/2019jc015807
14. Zhou, J. et al. The impact of dissolved organic carbon and bacterial respiration on pCO2 in experimental sea ice. *Progress in Oceanography* **141**, 153–167 (2016). https://doi.org/10.1016/j.pocean.2015.12.005
15. Brown, K. A. et al. Inorganic carbon system dynamics in landfast Arctic sea ice during the early-melt period. *Journal of Geophysical Research: Oceans* **120**, 3542–3566 (2015). https://doi.org/10.1002/2014JC010620
16. Delille, B. et al. Southern Ocean CO2 sink: The contribution of the sea ice. *Journal of Geophysical Research: Oceans* **119**, 6340–6355 (2014). https://doi.org/10.1002/2014JC009941

17. Geilfus, N.-X. et al. Estimates of ikaite export from sea ice to the underlying seawater in a sea ice-seawater mesocosm. *Cryosphere* **10**, (2016). https://doi.org/10.5194/tc-10-2173-2016
18. Geilfus, N.-X. et al. Inorganic carbon dynamics of melt-pond-covered first-year sea ice in the Canadian Arctic. *Biogeosciences* **12**, 2047–2061 (2015). https://doi.org/10.5194/bg-12-2047-2015
19. Geilfus, N.-X. et al. Dynamics of pCO2 and related air-ice CO2 fluxes in the Arctic coastal zone (Amundsen Gulf, Beaufort Sea). *Journal of Geophysical Research: Oceans* **117**, 1–15 (2012). https://doi.org/10.1029/2011JC007118
20. Nomura, D. et al. CO2 flux over young and snow-covered Arctic pack ice in winter and spring. *Biogeosciences* **15**, 3331–3343 (2018). https://doi.org/10.5194/bg-15-3331-2018
21. Rysgaard, S. et al. Sea ice contribution to the air-sea CO2 exchange in the Arctic and Southern Oceans. *Tellus B* **63**, 823–830 (2011). https://doi.org/10.1111/j.1600-0889.2011.00571.x
22. Rysgaard, S., Glud, R. N., Sejr, M. K., Bendtsen, J. & Christensen, P. B. Inorganic carbon transport during sea ice growth and decay: A carbon pump in polar seas. *Journal of Geophysical Research* **112**, C03016 (2007). https://doi.org/10.1029/2006JC003572
23. Crabeck, O., Delille, B., Moreau, S. & Fripiat, F. Gas dynamics in sea ice. in *Sea Ice: Its Physics, Chemistry, Biology, Geology and Societal Importance*, (2025). https://doi.org/10.1002/9781394213764.ch17
24. Dieckmann, G. S. et al. Ikaite (CaCO3*6H2O) discovered in Arctic sea ice. *The Cryosphere* **4**, 227–230 (2010). https://doi.org/10.5194/tc-4-227-2010
25. Dieckmann, G. S. et al. Calcium carbonate as ikaite crystals in Antarctic sea ice. *Geophysical Research Letters* **35**, L08501 (2008). https://doi.org/10.1029/2008GL033540
26. Nomura, D. et al. Characterization of ikaite (CaCO3 · 6H2O) crystals in first-year Arctic sea ice north of Svalbard. *Annals of Glaciology* **54**, 125–131 (2013). https://doi.org/10.3189/2013AoG62A034
27. Rysgaard, S. et al. Ikaite crystal distribution in winter sea ice and implications for CO2 system dynamics. *The Cryosphere* **7**, 707–718 (2013). https://doi.org/10.5194/tc-7-707-2013
28. Rysgaard, S. et al. Ikaite crystal distribution in Arctic winter sea ice and implications for CO 2 system dynamics. *The Cryosphere Discussions* **6**, 5037–5068 (2012). https://doi.org/10.5194/tcd-6-5037-2012
29. Crabeck, O. et al. Evidence of Freezing Pressure in Sea Ice Discrete Brine Inclusions and Its Impact on Aqueous-Gaseous Equilibrium. *Journal of Geophysical Research: Oceans* **124**, 1660–1678 (2019). https://doi.org/10.1029/2018JC014597
30. Crabeck, O. et al. Imaging air volume fraction in sea ice using non-destructive X-ray tomography. *The Cryosphere* **10**, 1125–1145 (2016). https://doi.org/10.5194/tc-10-1125-2016
31. Crabeck, O. et al. First “in situ” determination of gas transport coefficients (DO2, DAr, and DN2) from bulk gas concentration measurements (O2, N2, Ar) in natural sea ice. *Journal of Geophysical Research: Oceans* **119**, 6655–6668 (2014). https://doi.org/10.1002/2014JC009849

32. Loose, B. et al. Gas diffusion through columnar laboratory sea ice: Implications for mixed layer ventilation of CO2 in the seasonal ice zone. *Tellus B* **63**, 23–39 (2011). https://doi.org/10.1111/j.1600-0889.2010.00506.x
33. Zhou, J. et al. Physical and biogeochemical properties in landfast sea ice (Barrow, Alaska): Insights on brine and gas dynamics across seasons. *Journal of Geophysical Research: Oceans* **118**, 3172–3189 (2013). https://doi.org/10.1002/jgrc.20232
34. Grimm, R., Notz, D., Glud, R. N., Rysgaard, S. & Six, K. D. Assessment of the sea-ice carbon pump: Insights from a three-dimensional ocean-sea-ice-biogeochemical model (MPIOM/HAMOCC). *Elementa: Science of the Anthropocene* **4**, 000136 (2016). https://doi.org/10.12952/journal.elementa.000136
35. Moreau, S. et al. Assessment of the sea-ice carbon pump: Insights from a three-dimensional ocean-sea-ice biogeochemical model (NEMO-LIM-PISCES). *Elementa: Science of the Anthropocene* **4**, 000122 (2016). https://doi.org/10.12952/journal.elementa.000122
36. Richaud, B. et al. Underestimation of oceanic carbon uptake in the Arctic Ocean: ice melt as predictor of the sea ice carbon pump. *The Cryosphere* **17**, 2665–2680 (2023). https://doi.org/10.5194/tc-17-2665-2023
37. Papakyriakou, T. N. & Miller, L. A. Springtime CO2 exchange over seasonal sea ice in the Canadian Arctic Archipelago. *Annals of Glaciology* **52**, 215–224 (2011). https://doi.org/10.3189/172756411795931534
38. Semiletov, I., Makshtas, A., Akasofu, S.-I. & Andreas, E. L. Atmospheric CO2 balance: The role of Arctic sea ice. *Geophysical Research Letters* **31**, L05121 (2004). https://doi.org/10.1029/2003GL017996
39. Butterworth, B. J. & Else, B. G. T. Dried, closed-path eddy covariance method for measuring carbon dioxide flux over sea ice. *Atmospheric Measurement Techniques* **11**, 6075–6090 (2018). https://doi.org/10.5194/amt-11-6075-2018
40. Watts, J. et al. Impact of sea ice on air-sea CO2 exchange – A critical review of polar eddy covariance studies. *Progress in Oceanography* **201**, 102741 (2022). https://doi.org/10.1016/j.pocean.2022.102741
41. Miller, L. A. et al. Methods for biogeochemical studies of sea ice: The state of the art, caveats, and recommendations. *Elementa: Science of the Anthropocene* **3**, 000038 (2015). https://doi.org/10.12952/journal.elementa.000038
42. Delille, B., Jourdain, B., Borges, A. V., Tison, J.-L. & Delille, D. Biogas (CO2, O2, dimethylsulfide) dynamics in spring Antarctic fast ice. *Limnology and Oceanography* **52**, 1367–1379 (2007). https://doi.org/10.4319/lo.2007.52.4.1367
43. Moreau, S. et al. Drivers of inorganic carbon dynamics in first-year sea ice: A model study. *Journal of Geophysical Research: Oceans* **120**, 471–495 (2015). https://doi.org/10.1002/2014JC010388
44. Nomura, D., Yoshikawa-Inoue, H. & Toyota, T. The effect of sea-ice growth on air-sea CO2 flux in a tank experiment. *Tellus, Series B: Chemical and Physical Meteorology* **58**, 418–426 (2006). https://doi.org/10.1111/j.1600-0889.2006.00204.x
45. Nomura, D., Eicken, H., Gradinger, R. & Shirasawa, K. Rapid physically driven inversion of the air-sea ice CO2 flux in the seasonal landfast ice off Barrow,

Alaska after onset of surface melt. *Continental Shelf Research* **30**, 1998–2004 (2010). https://doi.org/10.1016/j.csr.2010.09.014
46. Dutch, V. R. et al. The Arctic Ocean CO2 Sink: Trends, Uncertainties, and the Impact of Sea Ice. *Global Biogeochemical Cycles* **39**, e2025GB008576 (2025). https://doi.org/10.1029/2025GB008576
47. Gray, A. R. et al. Autonomous Biogeochemical Floats Detect Significant Carbon Dioxide Outgassing in the High-Latitude Southern Ocean. *Geophysical Research Letters* **45**, 9049–9057 (2018). https://doi.org/10.1029/2018GL078013
48. Hauck, J. et al. The Southern Ocean Carbon Cycle 1985–2018: Mean, Seasonal Cycle, Trends, and Storage. *Global Biogeochemical Cycles* **37**, e2023GB007848 (2023). https://doi.org/10.1029/2023GB007848
49. Yasunaka, S. et al. An Assessment of CO2 Uptake in the Arctic Ocean From 1985 to 2018. *Global Biogeochemical Cycles* **37**, e2023GB007806 (2023). https://doi.org/10.1029/2023GB007806
50. Yasunaka, S. et al. Arctic Ocean CO2 uptake: an improved multiyear estimate of the air–sea CO2 flux incorporating chlorophyll a concentrations. *Biogeosciences* **15**, 1643–1661 (2018). https://doi.org/10.5194/bg-15-1643-2018
51. Sejr, M. K. et al. Air–sea flux of CO2 in arctic coastal waters influenced by glacial melt water and sea ice. *Tellus B: Chemical and Physical Meteorology* **63**, 815 (2011). https://doi.org/10.1111/j.1600-0889.2011.00540.x
52. Geilfus, N.-X. et al. First estimates of the contribution of CaCO3 precipitation to the release of CO2 to the atmosphere during young sea ice growth. *Journal of Geophysical Research: Oceans* **118**, 244–255 (2013). https://doi.org/10.1029/2012JC007980
53. Fischer, M. Sea ice and the air-sea exchange of CO2. (Universität Bremen, 2013).
54. Nomura, D., Granskog, M. A., Assmy, P., Simizu, D. & Hashida, G. Arctic and Antarctic sea ice acts as a sink for atmospheric CO2 during periods of snowmelt and surface flooding. *Journal of Geophysical Research: Oceans* **118**, 6511–6524 (2013). https://doi.org/10.1002/2013JC009048
55. Barber, D. et al. Frost flowers on young Artic sea ice: The climatic, chemical and microbial significance of an emerging ice type. *Journal of Geophysical Research D: Atmospheres* **119**, 11,593-11,612 (2014). https://doi.org/10.1002/2014JD021736
56. Geilfus, N.-X., Delille, B., Tison, J.-L., Lemes, M. & Rysgaard, S. Gas dynamics within landfast sea ice of an Arctic fjord (NE Greenland) during the spring–summer transition. *Elementa: Science of the Anthropocene* **11**, 00056 (2023).
⚠ DOI not provided in your correction list
57. Nomura, D. et al. CO2 flux measurements by chambers on sea ice during expedition PS122 (MOSAiC Legs 1−5) to the central Arctic in October 2019−September 2020. *PANGAEA* https://doi.org/10.1594/PANGAEA.966833 (2024).
58. Prytherch, J. et al. Central Arctic Ocean surface–atmosphere exchange of CO2 and CH4 constrained by direct measurements. *Biogeosciences* **21**, 671–688 (2024). https://doi.org/10.5194/bg-21-671-2024
59. Geilfus, N.-X. et al. Sea ice pCO2 dynamics and air–ice CO2 fluxes during the Sea Ice Mass Balance in the Antarctic (SIMBA) experiment – Bellingshausen Sea,

Antarctica. *The Cryosphere* **8**, 2395–2407 (2014). https://doi.org/10.5194/tc-8-2395-2014

60. Van der Linden, F. Autumn to spring inorganic carbon processes in pack and landfast sea ice in the Ross Sea, Antarctica. (Université de Liège & Université Libre de Bruxelles, 2021).
61. Nomura, D., Yoshikawa-Inoue, H., Toyota, T. & Shirasawa, K. Effects of snow, snowmelting and refreezing processes on air-sea-ice CO2 flux. *Journal of Glaciology* **56**, 262–270 (2010). https://doi.org/10.3189/002214310791968548
62. Fay, A. R. & McKinley, G. A. Global open-ocean biomes: mean and temporal variability. *Earth System Science Data* **6**, 273–284 (2014). https://doi.org/10.5194/essd-6-273-2014
63. Colbeck, S. C. Air Movement in Snow Due to Windpumping. *Journal of Glaciology* **35**, 209–213 (1989). https://doi.org/10.3189/S0022143000004524
64. Butterworth, B. J. et al. Annual carbon dioxide flux over seasonal sea ice in the Canadian Arctic. *EGUsphere* 1–30 (2025). https://doi.org/10.5194/egusphere-2025-1802
65. Meier, W. N. & Stroeve, J. An Updated Assessment of the Changing Arctic Sea Ice Cover. *Oceanography* **35**, 10–19 (2022). https://doi.org/10.5670/oceanog.2022.114
66. Silvano, A. et al. Rising surface salinity and declining sea ice: A new Southern Ocean state revealed by satellites. *Proc. Natl. Acad. Sci. U.S.A.* **122**, e2500440122 (2025). https://doi.org/10.1073/pnas.2500440122
67. Galley, R. J. et al. Micrometeorological and Thermal Control of Frost Flower Growth and Decay on Young Sea Ice. *Arctic* **68**, 79 (2015).https://doi.org/10.14430/arctic4457
68. EUMETSAT OSI SAF, Global sea ice concentration interim climate data record (SSMIS) (v3.0, 2022), OSI-430-a, doi:10.15770/EUM_SAF_OSI_0014
69. Niehaus, H. et al. Melt pond fractions on Arctic summer sea ice retrieved from Sentinel-3 satellite data with a constrained physical forward model. *The Cryosphere* **18**, 933–956 (2024). https://doi.org/10.5194/tc-18-933-2024

**Editorial summary:** A bipolar compilation of air-sea ice $CO_2$ fluxes shows that sea ice emits $CO_2$ in winter and absorbs it in summer. Annually, the sea ice represents a small net source of 2 to 4 Tg C per year for each polar ocean, negligible relative to total open-ocean carbon uptake.

**Peer review information:** *Nature Communications* thanks Elizabeth Jones, Xiang Yang, and the other, anonymous, reviewer(s) for their contribution to the peer review of this work. A peer review file is available.